Apoptosis (2021) 26:83–95
https://doi.org/10.1007/s10495-020-01651-z

Fluorizoline-induced apoptosis requires prohibitins in nematodes and human cells

José Saura-Esteller[1] · Ismael Sánchez-Vera[1] · Sonia Núñez-Vázquez[1] · Judith Jabalquinto-Carrasco[1] · Ana M. Cosialls[1] · Lorena Mendive-Tapia[2] · Dmytro Kukhtar[3] · Manuel D. Martínez-Bueno[4,5] · Rodolfo Lavilla[2] · Julián Cerón[3] · Marta Artal-Sanz[4,5] · Gabriel Pons[1] · Daniel Iglesias-Serret[1,6] · Joan Gil[1]

Accepted: 11 December 2020 / Published online: 2 January 2021

Abstract

We previously showed that fluorizoline, a fluorinated thiazoline compound, binds to both subunits of the mitochondrial prohibitin (PHB) complex, PHB1 and PHB2, being the expression of these proteins required for fluorizoline-induced apoptosis in mouse embryonic fibroblasts. To investigate the conservation of this apoptotic mechanism, we studied the effect of PHB downregulation on fluorizoline activity on two human cell lines, HEK293T and U2OS. Then, we asked whether PHBs mediate the effect of fluorizoline in a multicellular organism. Interestingly, reduced levels of PHBs in the human cells impaired the induction of apoptosis by fluorizoline. We observed that fluorizoline has a detrimental dose-dependent effect on the development and survival of the nematode model *Caenorhabditis elegans*. Besides, such effects of fluorizoline treatment in living nematodes were absent in PHB mutants. Finally, we further explored the apoptotic pathway triggered by fluorizoline in human cell lines. We found that the BH3-only proteins NOXA, BIM and PUMA participate in fluorizoline-induced apoptosis and that the induction of NOXA and PUMA is dependent on PHB expression.

Keywords Prohibitins · Fluorizoline · Apoptosis · *C. elegans*

Introduction

One of the main alterations driving the processes of tumorigenesis, malignization and tumour resistance to treatment is cell death resistance [1]. Although resistance to cell death can be caused by multiple mechanisms, mutations in the tumour suppressor p53 are found in more than 50% of the tumours [2]. Thus, the development of drugs that can cause cell death in a p53-independent manner is of key importance.

In previous studies, we described the synthesis of a new family of compounds, fluorinated thiazolines, that could trigger apoptosis independently of p53 mutational status [3]. Among this family of compounds we focused on the analysis of fluorizoline, due to its higher pro-apoptotic activity. fluorizoline treatment results in the induction of apoptosis in all cancer cell lines with different origin analysed and, importantly, in primary cells from various haematological malignancies [3–6].

We demonstrated that fluorizoline specifically binds to prohibitins (PHB) 1 and PHB2 [3]. Depletion of PHBs in mouse embryonic fibroblasts (MEF) blocked the induction of apoptosis by this compound [7]. Different drugs interact with PHBs and show potential to treat various diseases [8]. PHBs are highly conserved proteins mainly located in the inner mitochondrial membrane (IMM), where they form large multimeric ring-like complexes, although they can also be found in the plasma membrane or in the nucleus [9–12]. PHBs are involved in multiple processes throughout the cell, including signal transduction in the plasma membrane, transcriptional regulation in the nucleus and control of several mitochondrial functions, such as mitochondrial protein quality control, maintenance of mitochondrial ultrastructure, stability of mitochondrial DNA or mitophagy [13–16].

Supplementary Information The online version contains supplementary material available at https://doi.org/10.1007/s10495-020-01651-z.

Daniel Iglesias-Serret and Joan Gil shares seniorco-authorship.

✉ Joan Gil
jgil@ub.edu

Extended author information available on the last page of the article

PHBs were first shown to prevent cell cycle progression (hence prohibitins), and since then they have been shown to prevent the growth of certain tumours [17, 18]. Despite this possible tumour suppressor role, other studies indicate that PHBs participate in cell growth and metastasis [19–21]. In accordance, PHB downregulation can impair cell proliferation and increase the sensitivity of the cell to undergo apoptosis [22]. Thus, the role of PHBs in the survival or induction of apoptosis of cancer cells remains controversial and might depend on the origin of the tumour [10].

In addition, we showed that fluorizoline-induced apoptosis uses the intrinsic apoptotic pathway and implies alterations in the expression of BCL-2 family proteins. The BH3-only proteins NOXA and BIM were found to participate in fluorizoline-induced apoptosis by the mitochondrial pathway in MEF and HeLa cells [7].

Here we analyse the importance of PHBs for fluorizoline-induced apoptosis in cell lines from human origin and in the multicellular organism *Caenorhabditis elegans*, which has been previously used to study the physiological role of PHBs [23]. Moreover, we further study the mechanism of action of fluorizoline and show that the BH3-only proteins NOXA and BIM, but also PUMA, can participate in the induction of apoptosis by this compound in two human cell lines.

Materials and methods

Reagents

Fluorizoline was synthesized as described previously [3]. Q-VD-OPh was purchased from R&D systems (Minneapolis, Minnesota, USA). CCCP was purchased from Sigma-Aldrich (Saint Louis, Missouri, United States). MitoTracker™ Deep Red FM was purchased from Thermo Scientific, (Waltham, Massachusetts, USA).

Cell lines culture

HEK293T and U2OS cells were grown in DMEM complemented with 10% FBS, 2 mM L-glutamine, 100 U/mL penicillin, and 100 ng/mL streptomycin (all from Biological Industries, Beit Haemek, Israel). All cell lines were maintained at 37 °C in a humidified atmosphere containing 5% CO_2.

Flow cytometry

Phosphatidylserine exposure was used to determine cell viability. Cells were washed with PBS, pelleted, and then incubated with annexin binding buffer containing Annexin V-APC (Becton Dickinson Biosciences, Franklin Lakes, New Jersey, USA) for 15 min in the dark. Then, samples were analysed by flow cytometry using FACSCanto and FACSDiva software (Becton Dickinson Biosciences). Data represent the percentage of non-apoptotic cells (Annexin V-negative).

Transient transfection

For RNA interference, cells were transfected using Lipofectamine RNAiMAX reagent (Thermo Fisher). DMEM was replaced with OptiMEM (Gibco, Thermo Fisher) and complexes were added into cells dropwise and incubated for 4–6 h and then replaced again by fresh DMEM. The specific small interference RNAs (siRNAs) used were *BAK* (HSS141354, HSS141355, HSS141356), *BAX* (HSS184085, HSS184086, HSS184087), *PUMA* (HSS146893, HSS146894, HSS146895), *PHB1* (HSS182281) and *PHB2* (HSS117606) (Thermo Fisher).

Cell line generation by CRISPR/Cas9

NOXA and BIM deficient pools of HEK293T and U2OS cells and *PHB2*$^{-/+}$ HEK293T cells were generated as described by Ran et al. [24]. We designed short guide RNAs (sgRNA) to target *NOXA* (5′-TCGAGTGTGCTACTCAACTC-3′), *BIM* (5′-CTCCAATACGCCGCAACTCT-3′) and *PHB2* (5´ TGGGTCGAGACAACACTCGC 3′) *loci*. These guides were cloned into the pSpCas9(BB)-2A-Puro vector (supplied by Adgene, Watertown, MA, USA), which encodes the guides under the regulation of an RNA polymerase III promoter, the Cas9 endonuclease and a puromycin resistance element. Cells were transfected with Lipofectamine LTX for 48 h and then treated with 5 µg/mL puromycin to select edited cells. Puromycin was removed 24 h after the treatment, and then cells were allowed to recover. For the selection of the *PHB2*$^{-/+}$ HEK293T clone, individual cells were sorted into 96-well plates containing 200 µL of complete medium/well using a FACSAria cell sorter (Becton Dickinson Biosciences).

Stable expression of shPHB

We generated lentiviral particles by transfecting HEK293T cells with the Tet-pLKO-puro vector containing the sequence of an antisense short hairpin RNA (shRNA) targeting *PHB2* (5′-GACAGAGAGGGCCAAGGACCTCGAGGTCCTTGGCCCTCTCTGTC-3′) transcribed under a doxycycline promoter. Furtherly, *PHB2*$^{-/+}$ HEK293T cells were infected with these viral particles and cells were selected for resistance with 5 µg/mL puromycin.

Western blot

Pelleted cells were lysed with Laemmli sample buffer and protein quantification was performed with the Micro BCA Protein Assay Reagent kit (Pierce, Rockford, Illinois, USA). 15–30 µg of the protein samples were reduced by the addition of DTT and then loaded into a polyacrylamide gel and a 125-mV current was applied. For the transfer, Immobilon-P membranes (Millipore, Billerica, Massachusetts, USA) were used. Membranes were blocked with 5% (w/v) non-fat milk in Tris-buffered saline with Tween® 20 and then incubated with the specific primary antibodies overnight at 4 °C. Then, primary antibodies were removed, and membranes were incubated with secondary antibodies conjugated with horseradish peroxidase system (from GE Healthcare, Amersham, United Kingdom). Antibody binding was detected using enhanced chemiluminescence detection (GE Healthcare). The primary antibodies used were PHB1 (H-80, Santa Cruz, Dallas, Texas, USA), PHB2 (07-234, Millipore, Burlington, Massachusetts, USA), α-Tubulin (CP06, Millipore), PARP (9542, Cell Signalling technology, Danvers, Massachusetts, USA), Cleaved caspase 3 (67341A, Pharmingen, Beckton Dickinson), β-Actin (A5441, Sigma-Aldrich), BAK (06-536, Millipore), BAX (sc-493, Santa Cruz), OPA1 (612607, BD Biosciences) NOXA (ab13654, Abcam, Cambridge, United Kingdom), PUMA (4976, Cell Signalling), BIM (2933, Cell Signalling) and BCL-X_L (B22630, Becton Dickinson Biosciences).

Caenorhabditis elegans maintenance and treatment with fluorizoline

Bristol N2 was used as wild type (WT) strain and MRS56: *phb-2*(*tm2998*)/mln1[*dpy-10(e128)* mIs14(*Pmyo-2*::GFP)]II as *phb-2* deletion mutants. Worms were cultured following standard maintenance conditions [25]. Briefly, worms were maintained in nematode growth media (NGM) agar plates seeded with OP50 strain of *Escherichia coli* as food source at 20 °C.

For fluorizoline treatment, 175 µL of 20× concentrated drug was added on top of 35-mm NGM agar plates minimum 3 h prior to the worm addition, to let fluorizoline diffuse. Worms were synchronized following sodium hypochlorite treatment [26], once all L1 hatched, they were seeded onto fluorizoline plates and let at 20 °C until scoring was made. Pictures were taken with Zeiss Axiocam ERc 5-s camera (Zeiss, Oberkochen, Alemania) under the Zeiss Stemi 305 stereomicroscope at 10× and 40× magnification. Around 200 worms per condition were used in each of the 3 biological replicates. For survival assays, the number of alive worms were counted after two days on plate. For developmental assays, due to the different developmental timing of *phb-2* mutants, L4 stage worms were counted when animals reached the L4 larval stage in the respective control plates. For WT animals L4s were scored on the second day an on the fourth day for *phb-2* mutants.

Worm sorting

Synchronized L1 larvae were sorted using the flow cytometer COPAS (Complex Object Parametric Analyzer and Sorter) Biosort system. A sheath flow rate of 9.5 mL/min and worm concentration of 20–40 events/sec was maintained during sorting. To select homozygous *phb-2* deletion animals (non-GFP in the pharynx) from a mixed population of balanced heterozygous animals (GFP expression in the pharynx), green Peak Width vs. green Peak Height parameters was viewed, to enable the visualization of the different populations of worms. Non-GFP animals were sorted. WT N2 animals were also sorted to keep both strains under exactly the same conditions. Homozygous PHB deletion mutants from balanced heterozygous mothers develop into sterile adults due to maternal contribution [27].

Reverse transcriptase multiplex ligation-dependent probe amplification (RT-MLPA)

SALSA MLPA KIT (R011-C1) from MRC-Holland (Amsterdam, The Netherlands) was used to analyse relative mRNA expression of apoptosis-related genes. For these experiments, 200 ng RNA were reverse transcribed into cDNA with the specific primers. cDNA was annealed overnight at 60 °C to the RT-MLPA probe mix and, after that, oligonucleotides were ligated with Ligase-65 (MRC Holland, Amsterdam, Netherlands) and incubated at 54 °C for 15 min. PCR of the products was performed with FAM-labelled primers (35 cycles, 30 s at 95 °C; 30 s at 60 °C, and 1 min at 72 °C). The amplification products were separated by capillary electrophoresis on a 48-capillary ABI-Prism 3730 Genetic Analyzer (Applied Biosystems, California, USA). Coffalyser software (MRC Holland) was used to determine peak area. mRNA peak values are represented relative to total mRNA to normalise for variations of the intensity between samples. β-2-Microglobulin expression was used for normalisation.

Statistical analyses

Statistical analyses were performed with GraphPad Prism 6.0c Software Inc (Graph Pad Software, San Diego, California, USA). Results are represented by mean ± standard deviation (SD) or standard error of the mean (SEM) of at least three independent experiments unless stated otherwise. For simple comparisons, two-tailed Student's t test was used and for multiple comparisons two tailed ANOVA with Tukey's post-hoc test. P values inferior to 0.05 were considered statistically significant ($*p < 0.05$; $**p < 0.01$; $***p < 0.001$).

Results

PHBs are required for fluorizoline-induced apoptosis in human cell lines

Previous results from our group, using either conditional knock-outs (KOs) or siRNA-mediated downregulation of PHBs, indicated that reduction of PHB expression conferred MEF resistance to fluorizoline-treatment [7]. We sought to study which was the effect of PHB downregulation in cell lines from human origin. We decided to use human embryonic kidney (HEK293T) and human osteosarcoma (U2OS) cell lines due to their good transfection efficiency, which should allow us to strongly reduce PHB protein levels. Although PHB1 and PHB2 have been described to be interdependent at the protein level [22], we decided to use specific siRNAs against both proteins simultaneously to ensure an efficient reduction of PHB expression.

First, we treated HEK293T and U2OS cells with fluorizoline and with the inactive compound 2a [3]. As expected, fluorizoline but not compound 2a, reduced cell viability in both cell lines (Fig. 1a, b) HEK293T and U2OS cells were transfected with siRNAs against *PHB1* and *PHB2* for 72 h and then treated with fluorizoline. RNA interference effectively reduced PHB expression in both cell lines (Fig. 1c, d, f, g). Downregulation of PHBs in HEK293T and U2OS cells caused a slight, not significant, decrease in basal cell viability (Fig. 1e, h). Importantly, fluorizoline-induced apoptosis was reduced in PHB-downregulated HEK293T and U2OS cells. Moreover, to further reduce the levels of PHBs we generated *PHB2*$^{-/+}$ HEK293T cells stably expressing short hairpin antisense against *PHB2* under the control of an inducible promoter regulated by doxycycline, asdescribed in the *Materials and Methods* section. According to the previous experiment, the reduction of PHB expression in *PHB2*$^{-/+}$ HEK293T cells after treatment with doxycycline resulted in a strong resistance to fluorizoline-induced apoptosis (Fig. 1j, k).

These results demonstrate the involvement of PHBs in fluorizoline-induced apoptosis in cell lines from human origin.

The effect of fluorizoline on *C. elegans* is mediated by PHBs

To further analyse the relevance of PHB expression for fluorizoline-induced apoptosis, we decided to study the effect of PHBs deletion in an animal. We selected the nematode *C. elegans* which had been previously used to investigate the function of PHBs in embryonic viability and lifespan [23]. First, WT L1 larvae (N2 Bristol strain) were treated with different doses of fluorizoline to analyse whether this compound had an effect on worm development and survival. We found a severe reduction in worm survival when these animals were exposed to fluorizoline at concentrations higher than 1 µM, and little or no effect at lower concentrations. Overall, fluorizoline treatment caused defects in worm development at mild doses and lethality and growth arrest at the highest doses assessed (Fig. 2a).

We analysed the effect of phb-2 deletion (*phb-2*(*tm2998*) allele) on the worm lethality and growth defects caused by fluorizoline. WT and phb-2 mutant worms, selected as described previously [27] and in *Materials and Methods*, were treated with fluorizoline for up to 4 days. Due to the different growth rates of WT and *phb-2*(*tm2998*) animals, worm development was scored at the time when untreated worms reached the L4 larval stage, i.e. after 48 and 96 h, respectively. The effects of fluorizoline on worm survival and developmental growth were significantly reduced in *phb-2*-depleted worms (Fig. 2b, c).

Thus, fluorizoline treatment affects the survival and growth of *C. elegans*, and this effect is prevented in the absence of the PHB complex.

Fluorizoline activates apoptotic cell death through the mitochondrial pathway

Once we had established the relevance of PHBs for the induction of apoptosis in HEK293T and U2OS cell lines, we aimed to characterize the mechanism of apoptosis induction by fluorizoline in these two cell lines.

To study whether caspase inhibition could prevent fluorizoline-induced cell death in these two cell lines, we pretreated HEK293T and U2OS cell lines with the pan-caspase inhibitor Q-VD-OPh. Cells were pre-treated with Q-VD-OPh and then treated with fluorizoline for 24 h. fluorizoline treatment resulted in cleavage of the well-known markers of apoptosis, poly (ADP-ribose) polymerase (PARP) and caspase 3 (Fig. 3a, e), and loss of cell viability in a dose-dependent manner (Fig. 3b, f). Q-VD-OPh pre-treatment prevented the cleavage of PARP and caspase 3, as well as the loss of viability induced by fluorizoline in both cell lines, further indicating that fluorizoline triggers apoptosis in HEK293T and U2OS cell lines.

We downregulated *BAX* and *BAK* in HEK293T and U2OS to test whether fluorizoline required their expression to trigger apoptosis in these cell lines. Cells were transfected with specific siRNAs against *BAX* and *BAK* for 48 h and then treated with fluorizoline for 24 h. A clear reduction in BAX and BAK protein levels could be observed by western blot (Fig. 3c, g). As expected, lower levels of BAX and BAK in these cells caused increased resistance to fluorizoline-induced apoptosis (Fig. 3d, h). In HEK293T cells, downregulation of BAK was not effective in preventing fluorizoline-induced apoptosis, indicating that BAX plays a predominant

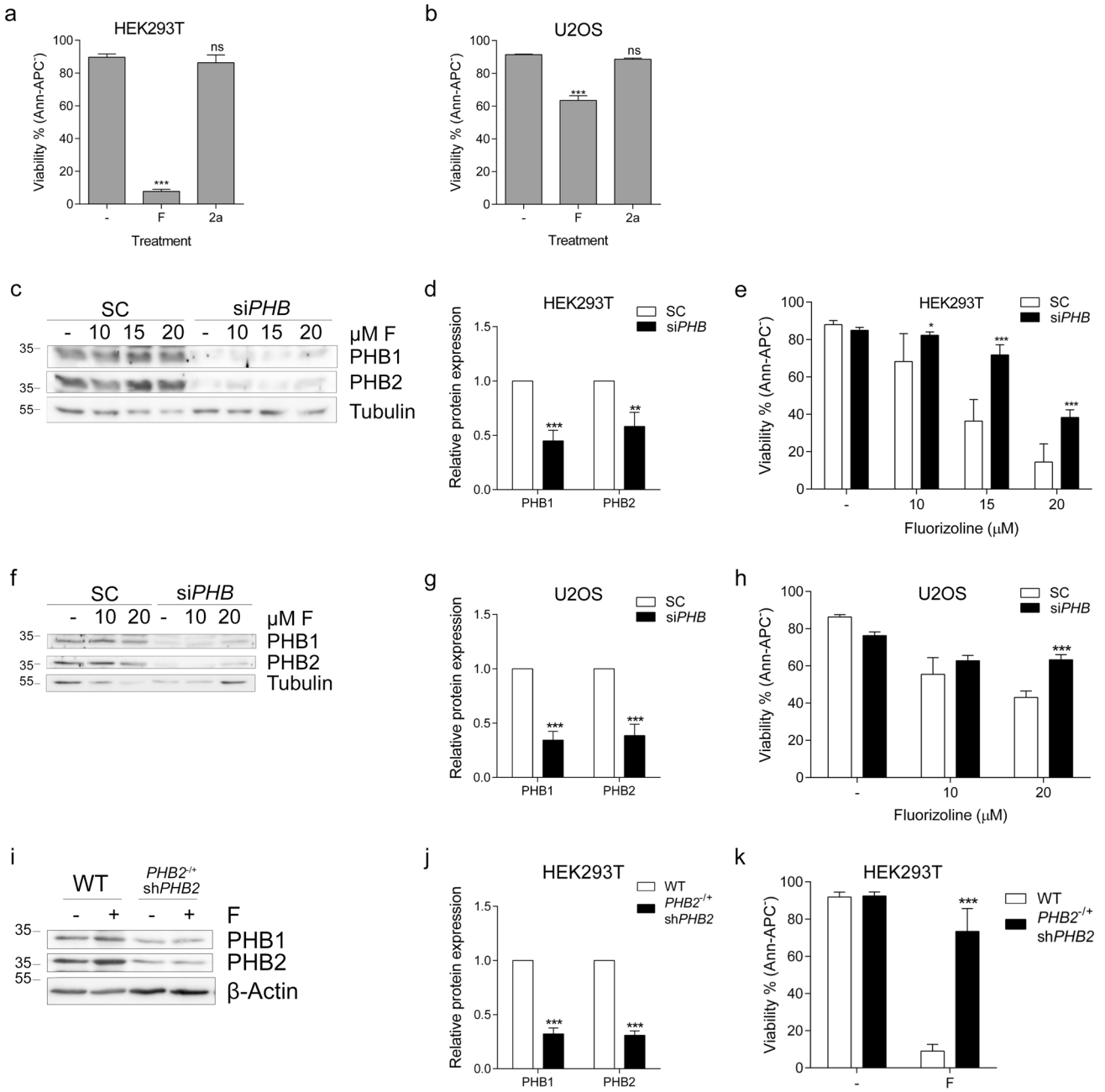

Fig. 1 PHBs are required for fluorizoline-induced apoptosis in human cell lines. **a**, **b** HEK293T and U2OS cells were treated with either 15 µM or 20 µM fluorizoline (F) and compound 2a respectively. **c**, **e** HEK293T and **f-h** U2OS cells were transfected with scramble (SC) or *PHB1* and *PHB2* (si*PHB*) siRNA for 72 h. Afterwards, cells were treated with the indicated doses of fluorizoline (F) for 24 h. **i**, **k** *PHB2*$^{-/+}$ HEK293T cells stably expressing an antisense shRNA against *PHB2* under the control of doxycycline were either left untreated or treated with 0.5 µg/mL doxycycline for 96 h and then left untreated or treated with 15 µM fluorizoline (F) for 24 h. **c**, **f**, **i** Protein levels were analysed by western blot. α-Tubulin and β-Actin were used as loading controls. **d**, **g**, **j** Untreated si*PHB* and sh*PHB2* band intensity was quantified and it is expressed relative to its respective SC or WT. **a**, **b**, **e**, **h**, **k** Viability was measured by flow cytometry and it is expressed as the mean ± SEM (n ≥ 3) of the percentage of non-apoptotic cells (annexin V-negative). *$p < 0.05$; **$p < 0.01$; ***$p < 0.001$; si*PHB vs.* SC and sh*PHB2 vs.* WT

role in the permeabilization of mitochondria in this cell line (Fig. 3c). In U2OS cells, we found increased resistance to fluorizoline treatment when either BAX and BAK were downregulated individually (Fig. 3h).

Additionally, we analysed the effect of fluorizoline treatment on mitochondrial membrane potential and OPA1 cleavage. To analyse the cleavage OPA1 we treated HEK293T and U2OS cells with fluorizoline for 6 or 24 h in the presence

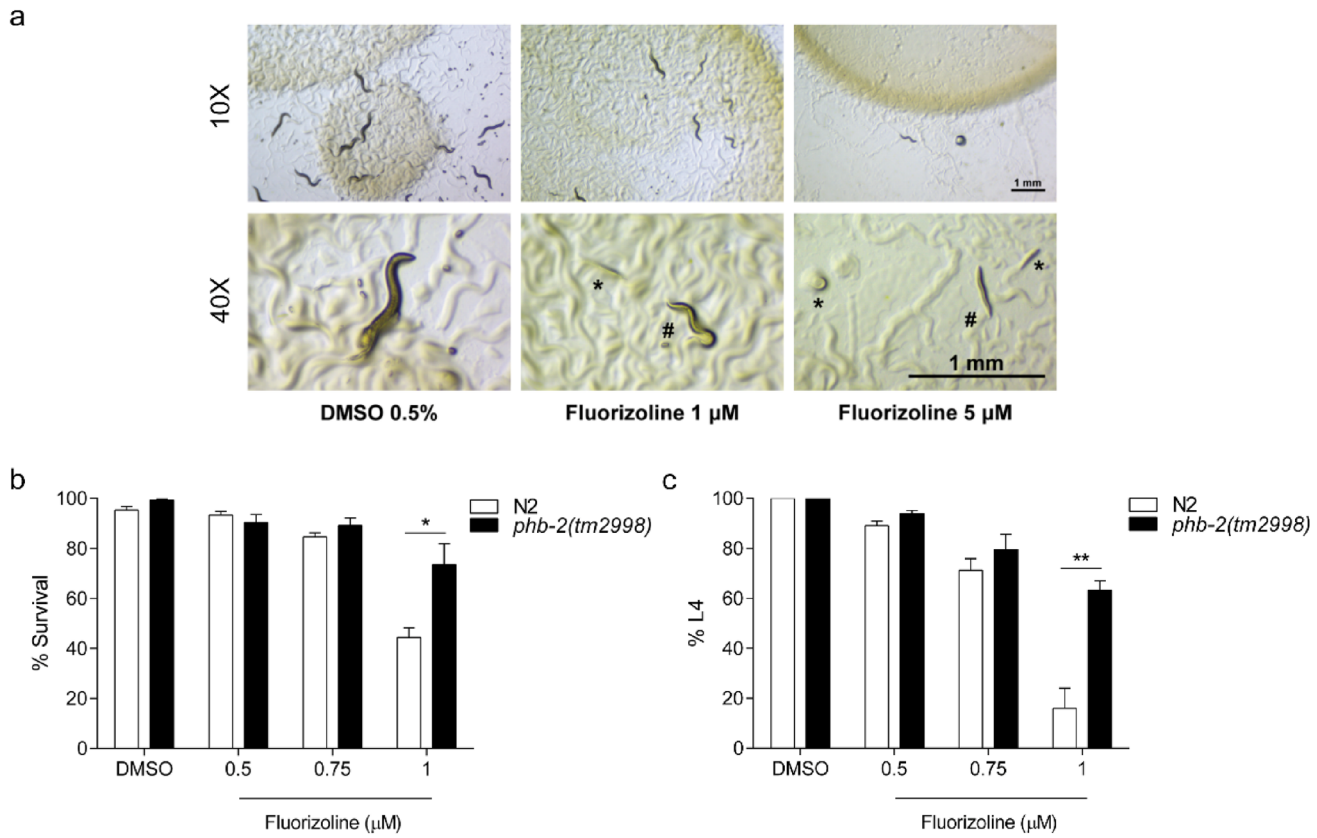

Fig. 2 The effect of fluorizoline on C. elegans is mediated by PHBs. **a** 25–30 L1 WT larvae were placed onto agar containing the indicated concentrations of either fluorizoline or 0.5% DMSO (corresponding to the higher dose of fluorizoline) as a negative control. Worms were maintained at 20 °C. Images were obtained 72 h post-seeding. These are representative images of three independent experiments. Lower, 10× magnification show different stages of growing defects upon fluorizoline treatment. Higher, 40× magnification show examples of dead (asterisk *) and arrested (hash #) larvae. **b**, **c** 50 WT N2 Bristol Strain (N2) or *phb-2*(*tm2998*) L1 larvae were placed in different nematode growth media plates containing either the indicated doses of fluorizoline or 0.05% DMSO (corresponding to the higher dose of fluorizoline) as a control plate. Worms were maintained at 20 °C. **b** Worm survival was scored 48 h after the start of the experiment. **c** Worm development was scored at the timepoint where untreated worms reached L4, i.e. 48 and 96 h after the start of the experiment for WT and *phb-2*(*tm2998*) worms, respectively. **b**, **c** Data are expressed as the mean ± SD of the percentage of worms (around 200 worms per condition in each of the 3 biological replicates). *$p < 0.05$; **$p < 0.01$; *phb-2 vs.* N2

of the pan-caspase inhibitor Q-VD-OPh, to avoid the effects of caspase activation. We observed partial loss of long isoforms of OPA1 (L-OPA1) 6 h after fluorizoline treatment and a more evident cleavage of L-OPA1 at 24 h in both cell lines (Fig. 4a, b). As previously described for Jurkat cells [7], treatment with fluorizoline for up to 8 h did not alter the accumulation of the potential sensitive dye MitoTracker Deep Red into the mitochondria, neither in HEK293T (Fig, 4d) nor in U2OS cells (Fig. 4c). On the contrary, the positive control CCCP significantly reduced MitoTracker Deep Red labelling in both cell lines.

Altogether these results indicate that HEK293T and U2OS cells treated with fluorizoline undergo BAX/BAK-dependent apoptotic cell death.

Fluorizoline modulates the expression of BIM, PUMA and NOXA to trigger apoptosis

To investigate which alterations in BCL-2 family members could be responsible for the activation of BAX and BAK in HEK293T and U2OS we decided to analyse the expression of the mRNA of some BCL-2 family members using reverse transcriptase multiplex ligation-dependent probe amplification (RT-MLPA).

In HEK293T cells, significant increases in *NOXA*, *BIM*, *PUMA* and *MCL-1L* and decreases in *BAX* mRNA levels were observed after treatment with fluorizoline for 24 h (Fig. 5a). In the case of U2OS cells, significant increases in *NOXA* and *MCL-1L* and reductions in *BAX* and *BCL-X_L* mRNA expression were detected (Fig. 5b).

We had previously observed that downregulation of PHBs in MEF resulted in complete blockage of the modulations of

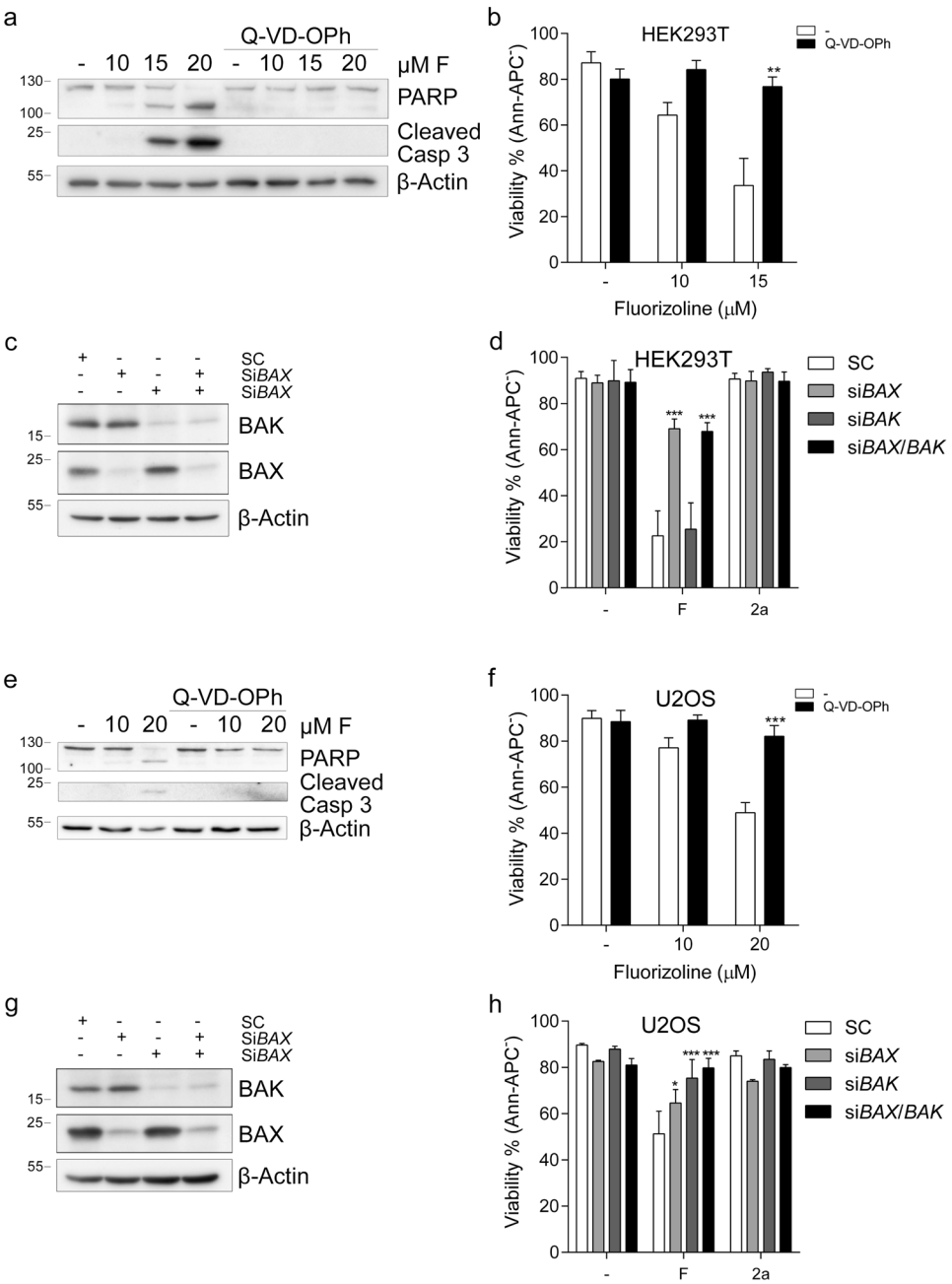

Fig. 3 Fluorizoline activates apoptotic cell death through the mitochondrial pathway. **a**, **b** HEK293T and **e**, **f** U2OS cells were left untreated or pre-treated with 20 µM Q-VD-OPh for 1 h. Then cells were treated with the indicated doses of fluorizoline (F) for 24 h. **c**, **d** HEK293T and **g**, **h** U2OS cells were transfected either with scramble (SC) or siRNA against *BAX* (si*BAX*), *BAK* (si*BAK*) or *BAX* and *BAK* (si*BAX*/*BAK*) for 48 h. Then cells were left untreated or treated with 15 µM or 20 µM of fluorizoline or compound 2a, respectively for 24 h. **b**, **d**, **f**, **h** Viability was measured by flow cytometry and it is expressed as the mean ± SEM (n = 3) of the percentage of non-apoptotic cells. *$p < 0.05$; **$p < 0.01$; ***$p < 0.001$; Q-VD-OPh vs. - or si*BAX*/*BAK vs.* SC. **a**, **c**, **e**, **g** Protein levels were analysed by western blot. β-actin was used as a loading control

mRNA expression produced by fluorizoline in that cell line [7]. We aimed to test whether PHB downregulation could also block the alterations on apoptosis-related genes in HEK293T and U2OS cells. To this end, we analysed mRNA expression of si*PHB*-transfected HEK293T and U2OS cell lines after fluorizoline treatment by RT-MLPA. Downregulation of PHBs in HEK293T resulted in a complete blockage of the inductions of *NOXA*, *PUMA* and *MCL-1L* mRNA after fluorizoline treatment, while *BIM* mRNA was increased independently of PHB downregulation (Fig. 5c). Similarly, the mRNA inductions of *NOXA* and *MCL-1L* were blocked by PHB downregulation in U2OS, while the reductions observed in *BCL-X*$_L$ and *BAX* expression were found to be independent on PHB expression (Fig. 5d). These RT-MLPA data indicate that some of the modulations of mRNA expression produced by fluorizoline treatment in these cell lines are dependent on PHB expression, while others can be triggered independently of PHBs.

Taking into consideration the modulations observed, we considered that the increases in *NOXA*, *BIM* and *PUMA* in HEK293T cells could be responsible for the activation of BAX and BAK. To test this hypothesis, we generated heterogenic pools of HEK293T cells with reduced *NOXA* (*NOXA*$^{-/-}$), *BIM* (*BIM*$^{-/-}$) and *NOXA*/*BIM*

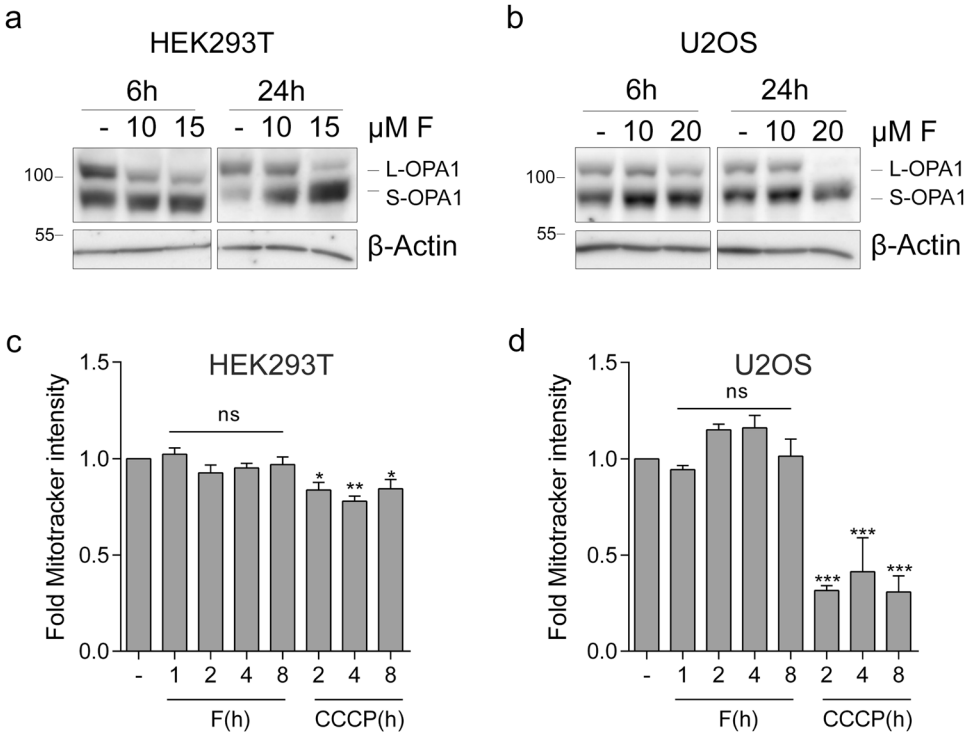

Fig. 4 Fluorizoline causes L-OPA1 cleavage but not loss of mitochondrial membrane potential. **a** HEK293T and **b** U2OS cells were pre-treated with 20 μM Q-VD-OPh for 1 h and then left untreated or treated with the indicated doses of fluorizoline for 6 or 24 h. **c** HEK293T and **d** U2OS cells were treated with 15 or 20 μM fluorizoline (F) or with 20 μM CCCP for the indicated time. 30 min prior to the end of the experiment cells were loaded with 100 nM MitoTracker Deep Red. **a**, **b** Protein levels were analysed by western blot. β-actin was used as a loading control. **c**, **d** Mitotracker Deep Red median fluorescence intensity was measured by flow cytometry and it is expressed as the mean ± SEM (n = 3) relative to untreated cells. $*p < 0.05$; $**p < 0.01$; $***p < 0.001$; each condition vs. -

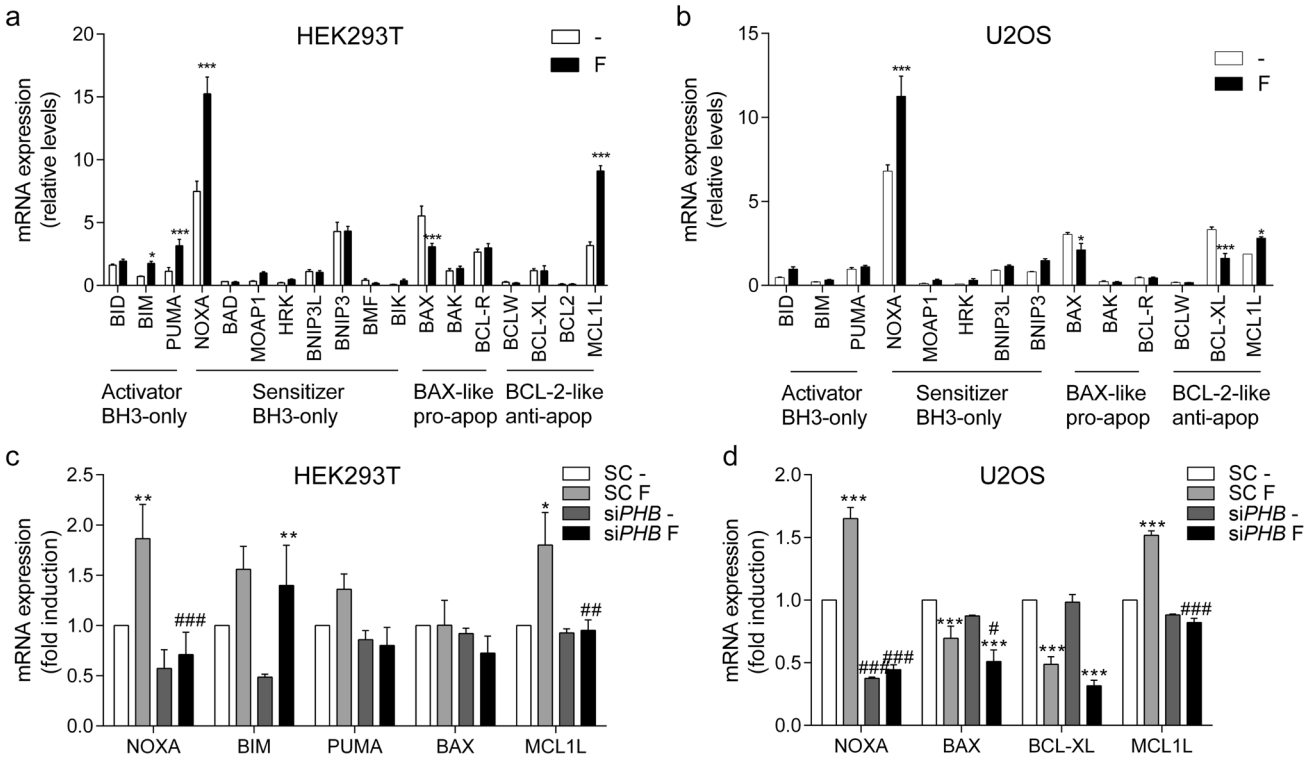

Fig. 5 Fluorizoline treatment results in modulations of the mRNA levels of different BCL-2 family members. **a** HEK293T and **b** U2OS cells were treated with 15 and 20 μM fluorizoline (F), respectively, for 24 h. **c** HEK293T and **d** U2OS cells were transfected with scramble (SC) or specific siRNAs against *PHB1* and *PHB2* (si*PHB*) for 72 h and then treated with 15 and 20 μM fluorizoline (F), respectively, for 24 h. Total mRNA was extracted and reverse-transcribed. Relative mRNA expression of 40 apoptosis-related genes was analysed by RT-MLPA. **a**, **b** Relative RNA expression and **c**, **d** fold induction referenced to the control (SC -) are expressed as the mean ± SEM (a, c n = 3; b, d n = 2) $*p < 0.05$; $**p < 0.01$; $***p < 0.001$; of F vs. -. $\#p < 0.05$; $\#\#p < 0.01$; $\#\#\#p < 0.001$; si*PHB vs.* SC

expression (*NOXA*$^{-/-}$/*BIM*$^{-/-}$) by CRISPR/*Cas9* technology (Fig. 6a). First, we treated WT, *NOXA*$^{-/-}$, *BIM*$^{-/-}$ and *NOXA*$^{-/-}$/*BIM*$^{-/-}$ HEK293T cells with fluorizoline and analysed the effect of the deletion of these two BH3-only proteins on cell viability. Deletion of *BIM* alone was enough to partially prevent fluorizoline-induced apoptosis in HEK293T cells (Fig. 6b). On the contrary, *NOXA* depletion had no effect on the decrease of cell viability caused by fluorizoline either alone or in combination with *BIM* depletion. Next, we transfected WT and *NOXA*$^{-/-}$/*BIM*$^{-/-}$ cells with specific siRNAs against *PUMA* for 48 h and then treated these cells with fluorizoline for 24 h. A partial downregulation of PUMA protein could be observed by western blot (Fig. 6c). WT cells transfected with si*PUMA* and *NOXA*$^{-/-}$/*BIM*$^{-/-}$ cells were slightly more resistant to fluorizoline treatment. Knockdown of *PUMA* in *NOXA*$^{-/-}$/*BIM*$^{-/-}$ further increased cell resistance against fluorizoline-induced apoptosis (Fig. 6d).

In U2OS cells, fluorizoline-induced apoptosis could be caused by a combination of increased *NOXA* and decreased *BCL-X*$_L$ expression. We generated heterogenic pools of cells with reduced *NOXA* expression. WT and *NOXA*$^{-/-}$ U2OS cells were treated with fluorizoline for 24 h and cell viability was assessed by flow cytometry. *NOXA*$^{-/-}$ cells were found to be more resistant to fluorizoline treatment than WT cells, indicating that NOXA protein increases are key for fluorizoline-induced apoptosis in this cell line (Fig. 7a, b). Moreover, we analysed BCL-X$_L$ protein expression after fluorizoline treatment and found a reduction of this protein after 24 h of treatment (Fig. 7c). This effect could be blocked by pre-treatment with Q-VD-OPh, indicating that this reduction is caused by the activation of caspases.

Thus, we have shown that BIM and PUMA in HEK293T cells and NOXA in U2OS cells are the most relevant BH3-only proteins involved in the induction of apoptosis after fluorizoline treatment. Altogether these results indicate that BH3-only involvement in fluorizoline-induced apoptosis is cell-type specific.

Discussion

In this study we further explore the relevance of PHBs as target proteins of the synthetic pro-apoptotic molecule fluorizoline using human cell lines and *C. elegans*. Moreover, we

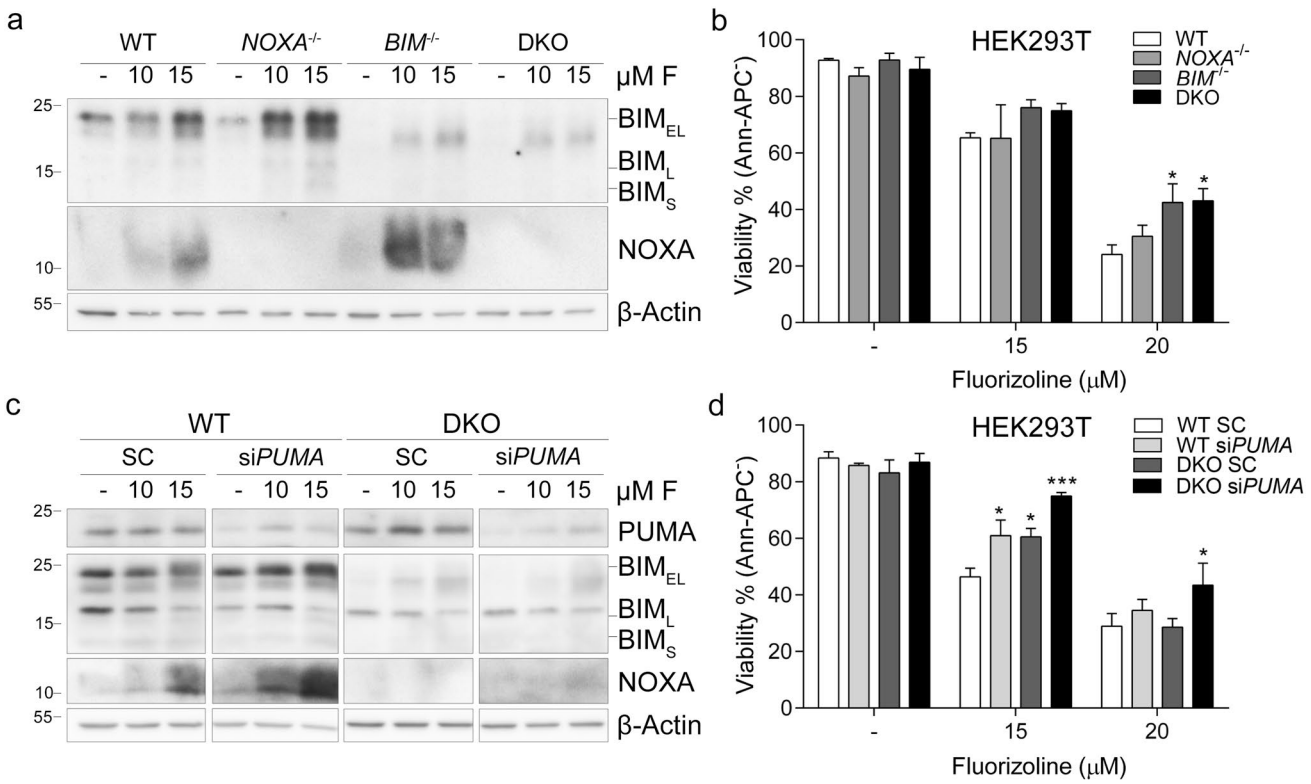

Fig. 6 Fluorizoline-induced apoptosis is mediated by BIM and PUMA in HEK293T cells. **a**, **b** WT, *NOXA*$^{-/-}$, *BIM*$^{-/-}$ and *NOXA*$^{-/-}$/*BIM*$^{-/-}$ (DKO) HEK293T cells were treated with the indicated doses of fluorizoline (F) for 24 h. **c**, **d** WT and DKO HEK293T cells were transfected with scramble (SC) or specific siRNA against *PUMA* (si*PUMA*) for 48 h and then treated with the indicated doses of fluorizoline (F) for 24 h. **a**, **c** Protein levels were analysed by western blot. β-actin was used as a loading control. *Unspecific band. **b**, **d** Viability was measured by flow cytometry and it is expressed as the mean ± SEM (n = 3) of the percentage of non-apoptotic cells (annexin V-negative). *$p < 0.05$; **$p < 0.01$; ***$p < 0.001$; Each condition vs. WT or WT SC

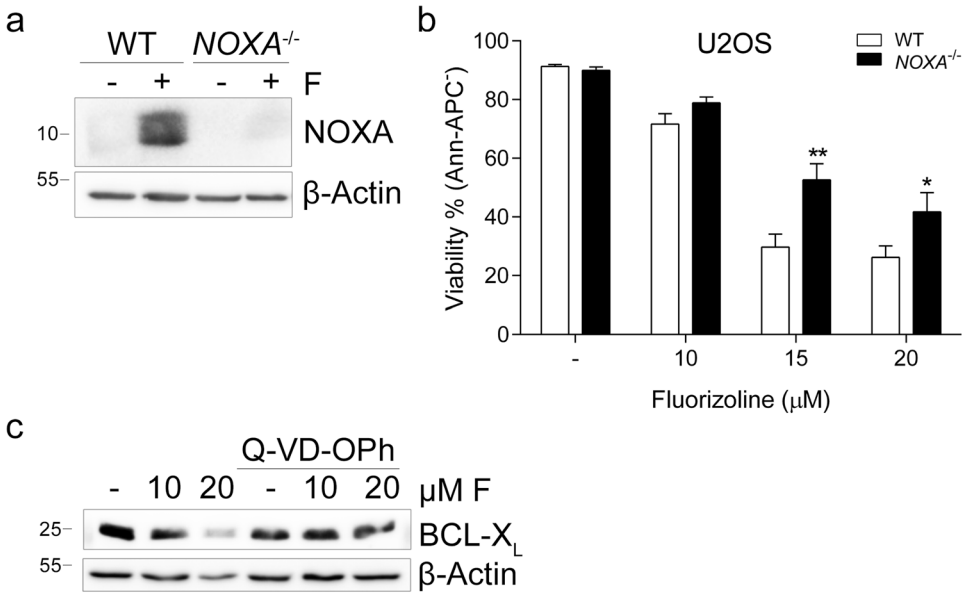

Fig. 7 Fluorizoline-induced apoptosis is mediated by NOXA in U2OS cells. **a**, **b** WT and *NOXA*$^{-/-}$ U2OS cells were treated with **a** 20 μM fluorizoline (F) or **b**, **c** with the indicated doses of fluorizoline (F) for 24 h. **c** WT cells were left untreated or pre-treated with 20 μM Q-VD-OPh for 1 h and then treated with the indicated doses of fluorizoline (F) for 24 h. **a**, **c** Protein levels were analysed by western blot. β-actin was used as a loading control. **b** Viability was measured by flow cytometry and it is expressed as the mean ± SEM (n = 3) of the percentage of non-apoptotic cells (annexin V-negative)

characterize fluorizoline-induced apoptosis and the modulations of BCL-2 family proteins leading to this induction. Finally, we show that the BH3-only proteins BIM, PUMA in HEK293T and NOXA in U2OS, respectively, can trigger the mitochondrial pathway of apoptosis.

Previous results from our group showed that fluorizoline could bind specifically to PHBs and that the reduction of the expression of these proteins in MEF strongly affected cell resistance to fluorizoline treatment [3, 7]. Here we show that PHB downregulation prevents fluorizoline-induced apoptosis in HEK293T and U2OS human cells and *C. elegans*. These results highlight the relevance of PHBs for the induction of apoptosis by fluorizoline. PHBs are highly conserved proteins, a trait that might explain that the effect of the downregulation of PHBs on fluorizoline-induced apoptosis is conserved in murine and human cell lines as well as and in *C. elegans*.

Fluorizoline treatment results in the induction of apoptosis in all cancer cell lines with different origin analysed and, importantly, in primary cells from various haematological malignancies [3–6]. However, fluorizoline is inactive in a murine model of chronic lymphocytic leukaemia [6]. Our results (data not shown) indicate that the lack of activity could be caused by the inability of fluorizoline to get the target cells when administered *in vivo* by intraperitoneal injection. It will be interesting to encapsulate fluorizoline to improve its bioavailability.

In *C. elegans*, PHB expression has been shown to regulate mitochondrial homeostasis, and RNA interference-mediated downregulation of PHBs has an impact on embryonic development and lifespan of these nematodes [23, 28]. A study aimed to describe mutations that resulted in resistance to the anti-mitotic drug hemiasterlin described a missense mutation in *PHB2* that led to resistance to multiple drugs even in heterozygous worms [29]. This resistance might be caused by mitochondrial disfunction resulting from the lack of proper activity of the PHB complex in the IMM, as drugs causing alterations in mitochondrial respiratory activity caused a similar effect [30]. Here we show that the PHB-binding drug fluorizoline is toxic for *C. elegans* at concentrations around 1 μM and this toxicity is reduced in PHB-depleted worms. Whether the observed resistance is caused by mitochondrial defects produced by PHB depletion remains an open possibility. However, this result is in line with the increased resistance of mammalian cells to fluorizoline-induced apoptosis after PHB downregulation, even when this downregulation has been shown to increase cell sensitivity to other pro-apoptotic drugs [22].

Fluorizoline activity relies on the activation of the intrinsic pathway of apoptosis caused by modulations of the expression of BH3-only proteins. We had shown that NOXA played a predominant role in the induction of apoptosis by fluorizoline in HeLa cells, as well as in hematologic primary cells, while downregulation of BIM had no impact on the viability of these cells [7]. In the case of MEF, we determined that individual KO of *Noxa* and *Bim* did not alter cell viability, whereas double KO of *Noxa* and *Bim* reduced the induction of apoptosis by fluorizoline. In the present study, we have confirmed the relevance of *NOXA* and *BIM* for the induction of apoptosis by this compound and that the involvement of these proteins is cell-type specific. Moreover, we have shown that PUMA can also participate in fluorizoline-induced apoptosis, as downregulation of this BH3-only protein can increase cell viability after fluorizoline treatment in HEK293T cells. Interestingly, PUMA is a BH3-only pro-apoptotic member that binds all anti-apoptotic members of

the BCL-2 family with a mechanism of control different of that of NOXA, which binds only MCL-1 [31]. Although *PUMA* mRNA was increased after fluorizoline treatment in HEK293T cells, its protein levels were not increased by fluorizoline unless NOXA and BIM were absent (Fig. 6c). Despite this, downregulation of PUMA in the presence of NOXA and BIM significantly reduced fluorizoline-induced apoptosis, suggesting that PUMA might participate in fluorizoline-induced apoptosis by other means than an increase in its protein levels. Of note, certain BH3-only proteins are increased when the expression of other is reduced, indicating a potential compensatory mechanism. Thus, we cannot exclude the participation of other BH3-only proteins in the absence of NOXA, BIM and PUMA. Depletion of BH3-only proteins either by CRISPR/*Cas9* or by siRNA-mediated downregulation led to partial blockage of the induction of apoptosis by fluorizoline. Previously we showed that fluorizoline could also cause induction of apoptosis through the activation of caspase 8 in $Bax^{-/-}/Bak^{-/-}$ MEF [7], an effect that could be also taking place in cells with depletion of BH3-only proteins. These results further highlight the cell-type specificity for BH3-only involvement in the response to fluorizoline treatment.

In conclusion, we observe that PHB expression is key for the pro-apoptotic activity of the PHB-binding compound fluorizoline in human embryonic and cancer cell lines as well as in *C. elegans*. Importantly, we have confirmed that treatment with fluorizoline results in activation of the mitochondrial pathway of apoptosis through modulations of the BH3-only proteins NOXA and BIM and demonstrated that PUMA can also participate in this process. How the interaction of fluorizoline with PHBs results in the induction of BH3-only proteins remains to be determined and will be matter of future studies. The elucidation of the mechanism of action of this compound will be important to establish future applications for fluorizoline or other PHB-binding compounds.

Acknowledgements We thank the CERCA Program/Generalitat de Catalunya for their institutional support. We also thank the Scientific and Technological Centers of Bellvitge Campus at the University of Barcelona.

Author contributions Conceptualization, JS-E, JC, MA-S, GP, DI-S and JG; Funding acquisition, RL, JC, MA-S and JG; Investigation, JS-E, JJ-C, DK, MDM-B and GP; Resources, LM-T and RL; Supervision, JG; Writing—original draft, JS-E, JC, MA-S, DI-S and JG; Writing—review & editing, IS-V, SN-V, JJ-C, AMC, LM-T, DK, MDM-B, RL and GP.

Funding This work was supported by grants from the Agencia Estatal de Investigación (Ministerio de Ciencia e Innovación), European Regional Development Fund (ERDF), the European Research Council, the Junta de Andalucía and the Instituto de Salud Carlos III (ISCIII) (SAF2017-83178-R to J.G.; PID2019-107991RB-I00 to R.L.; ERC-2011-StG-281691 and C2A ID: 42571/Exp: 70806 to M.A-S; PI15-00895 to J.C.). J.S-E and I.S-V are recipients of research fellowships from the Ministerio de Ciencia e Innovación. S.N-V is recipient of a research fellowship from Universitat de Barcelona. MD.M-B was supported by the Plan de Empleo Juvenil (EJP09) from the Junta de Anadalucía. D.K has a FI AGAUR fellowship from Generalitat de Catalunya.

Compliance with ethical standards

Conflict of interest The authors declare no conflict of interest.

References

1. Hanahan D, Weinberg RA (2011) Hallmarks of cancer: the next generation. Cell 144:646–674. https://doi.org/10.1016/j.cell.2011.02.013
2. Muller PAJ, Vousden KH (2013) P53 mutations in cancer. Nat Cell Biol 15:2–8
3. Pérez-Perarnau A, Preciado S, Palmeri CM et al (2014) A trifluorinated thiazoline scaffold leading to pro-apoptotic agents targeting prohibitins. Angew Chem Int Ed 53:10150–10154. https://doi.org/10.1002/anie.201405758
4. Pomares H, Palmeri CM, Iglesias-Serret D et al (2016) Targeting prohibitins induces apoptosis in acute myeloid leukemia cells. Oncotarget 7:64987–65000. https://doi.org/10.18632/oncotarget.11333
5. Cosialls AM, Pomares H, Iglesias-Serret D et al (2017) The prohibitin-binding compound fluorizoline induces apoptosis in chronic lymphocytic leukemia cells through the upregulation of NOXA and synergizes with ibrutinib, 5-aminoimidazole-4-carboxamide riboside or venetoclax. Haematologica 102:1587–1593. https://doi.org/10.3324/haematol.2016.162958
6. Wierz M, Pierson S, Chouha N et al (2018) The prohibitin-binding compound fluorizoline induces apoptosis in chronic lymphocytic leukemia cells ex vivo but fails to prevent leukemia development in a murine model. Haematologica 103:e154–e157
7. Moncunill-Massaguer C, Saura-Esteller J, Pérez-Perarnau A et al (2015) A novel prohibitin-binding compound induces the mitochondrial apoptotic pathway through NOXA and BIM upregulation. Oncotarget 6:41750–41765. https://doi.org/10.18632/oncotarget.6154
8. Wang D, Tabti R, Elderwish S et al (2020) Prohibitin ligands: a growing armamentarium to tackle cancers, osteoporosis, inflammatory, cardiac and neurological diseases. Cell Mol Life Sci. https://doi.org/10.1007/s00018-020-03475-1
9. Thuaud F, Ribeiro N, Nebigil CG, Désaubry L (2013) Prohibitin ligands in cell death and survival: mode of action and therapeutic potential. Chem Biol 20:316–331
10. Yang J, Li B, He QY (2018) Significance of prohibitin domain family in tumorigenesis and its implication in cancer diagnosis and treatment review-article. Cell Death Dis 9:580
11. Signorile A, Sgaramella G, Bellomo F, De Rasmo D (2019) Prohibitins: a critical role in mitochondrial functions and implication in diseases. Cells 8:71. https://doi.org/10.3390/cells8010071
12. Peng Y-T, Chen P, Ouyang R-Y, Song L (2015) Multifaceted role of prohibitin in cell survival and apoptosis. Apoptosis 20:1135–1149. https://doi.org/10.1007/s10495-015-1143-z
13. Wei Y, Chiang W-C, Sumpter R et al (2017) Prohibitin 2 is an inner mitochondrial membrane mitophagy receptor. Cell 168:224-238.e10. https://doi.org/10.1016/j.cell.2016.11.042
14. Hernando-Rodríguez B, Artal-Sanz M (2018) Mitochondrial quality control mechanisms and the PHB (Prohibitin). Complex Cells 7:238. https://doi.org/10.3390/cells7120238

15. Nijtmans LGJ, Artal Sanz M, Grivell LA, Coates PJ (2002) The mitochondrial PHB complex: roles in mitochondrial respiratory complex assembly, ageing and degenerative disease. Cell Mol Life Sci 59:143–155
16. Chowdhury I, Thompson WE, Welch C et al (2013) Prohibitin (PHB) inhibits apoptosis in rat granulosa cells (GCs) through the extracellular signal-regulated kinase 1/2 (ERK1/2) and the Bcl family of proteins. Apoptosis 18:1513–1525. https://doi.org/10.1007/s10495-013-0901-z
17. McClung JK, Danner DB, Stewart DA et al (1989) Isolation of a cDNA that hybrid selects antiproliferative mRNA from rat liver. Biochem Biophys Res Commun 164:1316–1322. https://doi.org/10.1016/0006-291X(89)91813-5
18. Liu P, Xu Y, Zhang W et al (2017) Prohibitin promotes androgen receptor activation in ER-positive breast cancer. Cell Cycle 16:776–784. https://doi.org/10.1080/15384101.2017.1295193
19. Cao Y, Liang H, Zhang F et al (2016) Prohibitin overexpression predicts poor prognosis and promotes cell proliferation and invasion through ERK pathway activation in gallbladder cancer. J Exp Clin Cancer Res. https://doi.org/10.1186/s13046-016-0346-7
20. Fu P, Yang Z, Bach LA (2013) Prohibitin-2 binding modulates insulin-like growth factor-binding protein-6 (IGFBP-6)-induced rhabdomyosarcoma cell migration. J Biol Chem 288:29890–29900. https://doi.org/10.1074/jbc.M113.510826
21. Chiu CF, Ho MY, Peng JM et al (2013) Raf activation by Ras and promotion of cellular metastasis require phosphorylation of prohibitin in the raft domain of the plasma membrane. Oncogene 32:777–787. https://doi.org/10.1038/onc.2012.86
22. Merkwirth C, Dargazanli S, Tatsuta T et al (2008) Prohibitins control cell proliferation and apoptosis by regulating OPA1-dependent cristae morphogenesis in mitochondria. Genes Dev 22:476–488. https://doi.org/10.1101/gad.460708
23. Sanz MA, Tsang WY, Willems EM et al (2003) The mitochondrial prohibitin complex is essential for embryonic viability and germline function in Caenorhabditis elegans. J Biol Chem 278:32091–32099. https://doi.org/10.1074/jbc.M304877200
24. Ran FA, Hsu PD, Wright J et al (2013) Genome engineering using the CRISPR-Cas9 system. Nat Protoc 8:2281–2308. https://doi.org/10.1038/nprot.2013.143
25. Brenner S (1974) The genetics of *Caenorabditis elegans*. Genetics. https://doi.org/10.1016/S0047-2484(78)80101-8
26. Porta-de-la-Riva M, Fontrodona L, Villanueva A, Cerón J (2012) Basic *Caenorhabditis elegans* methods: synchronization and observation. J Vis Exp. https://doi.org/10.3791/4019
27. Hernando-Rodríguez B, Erinjeri AP, Rodríguez-Palero MJ et al (2018) Combined flow cytometry and high-throughput image analysis for the study of essential genes in *Caenorhabditis elegans*. BMC Biol 16:36. https://doi.org/10.1186/s12915-018-0496-5
28. Artal-Sanz M, Tavernarakis N (2009) Prohibitin couples diapause signalling to mitochondrial metabolism during ageing in *C. elegans*. Nature 461:793–797. https://doi.org/10.1038/nature08466
29. Zubovych I, Doundoulakis T, Harran PG, Roth MG (2006) A missense mutation in *Caenorhabditis elegans* prohibitin 2 confers an atypical multidrug resistance. Proc Natl Acad Sci USA 103:15523–15528. https://doi.org/10.1073/pnas.0607338103
30. Zubovych IO, Straud S, Roth MG (2010) Mitochondrial dysfunction confers resistance to multiple drugs in *Caenorhabditis elegans*. Mol Biol Cell 21:956–969. https://doi.org/10.1091/mbc.E09-08-0673
31. Birkinshaw RW, Czabotar PE (2017) The BCL-2 family of proteins and mitochondrial outer membrane permeabilisation. Semin Cell Dev Biol 72:152–162

Affiliations

José Saura-Esteller[1] · Ismael Sánchez-Vera[1] · Sonia Núñez-Vázquez[1] · Judith Jabalquinto-Carrasco[1] · Ana M. Cosialls[1] · Lorena Mendive-Tapia[2] · Dmytro Kukhtar[3] · Manuel D. Martínez-Bueno[4,5] · Rodolfo Lavilla[2] · Julián Cerón[3] · Marta Artal-Sanz[4,5] · Gabriel Pons[1] · Daniel Iglesias-Serret[1,6] · Joan Gil[1]

José Saura-Esteller
Jsauraes@ub.edu

Ismael Sánchez-Vera
isanchezvera@ub.edu

Sonia Núñez-Vázquez
snunez@ub.edu

Judith Jabalquinto-Carrasco
jjabalquintocarrasco@gmail.com

Ana M. Cosialls
anamcosialls@ub.edu

Lorena Mendive-Tapia
lorena.mendive@gmail.com

Dmytro Kukhtar
dkukhtar@idibell.cat

Manuel D. Martínez-Bueno
mdmarbue@upo.es

Rodolfo Lavilla
rlavilla@ub.edu

Julián Cerón
jceron@idibell.cat

Marta Artal-Sanz
martsan@upo.es

Gabriel Pons
gpons@ub.edu

Daniel Iglesias-Serret
daniel.iglesias@umedicina.cat

[1] Departament de Ciències Fisiològiques, Facultat de Medicina i Ciències de la Salut, Universitat de Barcelona-IDIBELL (Institut d'Investigació Biomèdica de Bellvitge), L'Hospitalet de Llobregat, Barcelona, Spain

[2] Laboratory of Medical Chemistry, Faculty of Pharmacy and Food Sciences, Institute of Medicine (IBUB), University of Barcelona, Barcelona, Spain

[3] Modeling Human Diseases in C. Elegans Group. Genes, Disease and Therapy Program, IDIBELL (Institut d'Investigació Biomèdica de Bellvitge), L'Hospitalet de Llobregat, Barcelona, Spain

[4] Andalusian Center for Developmental Biology, Consejo Superior de Investigaciones Científicas/Junta de Andalucía, Universidad Pablo de Olavide, Seville, Spain

[5] Department of Molecular Biology and Biochemical Engineering, Universidad Pablo de Olavide, Seville, Spain

[6] Facultat de Medicina, Universitat de Vic-Universitat Central de Catalunya (UVic-UCC), Vic, Barcelona, Spain